

Article

Interfacial Reaction and Microstructure Evolution of Sn-9Zn/Ni(Cu) Solder Joints

Xuewei Zhu ¹ , Jian Peng ^{2,*}, Xiaofeng Wei ¹, Pengpeng Yan ¹ and Fu Wang ¹

¹ College of Mechanical and Electronic Engineering, Northwest A&F University, Yangling 712100, China; zwx_83614@163.com (X.Z.); wxf8412@nwfau.edu.cn (X.W.); yanpengpeng@nwfau.edu.cn (P.Y.); wangfu@nwfau.edu.cn (F.W.)

² School of Materials Science and Engineering, Central South University, Changsha 410083, China

* Correspondence: j.peng@csu.edu.cn; Tel.: +86-158-7410-1500

Received: 5 April 2019; Accepted: 22 May 2019; Published: 24 May 2019



Abstract: Sn-9Zn solder is a promising Pb-free solder, but it tends to form bulky intermetallic compounds (IMC) grains at the interface when soldered with common simple metal Cu or Ni substrates. Interfacial reaction between Sn-9Zn solder and Ni(Cu) solid solution substrates at 250 °C and 350 °C were systematically probed in this study. Results showed that when soldered at 250 °C, a Ni₅Zn₂₁ layer is formed at Sn-Zn/Ni-20Cu and Sn-Zn/Ni-40Cu joints; and Ni₂Sn₂Zn + Cu₅Zn₈ and Cu₅Zn₈ phases are formed in Sn-Zn/Ni-60Cu and Sn-Zn/Ni-80Cu joints, respectively. Fine-grained IMCs formed at the interface are formed even when the soldered time is prolonged to 16 h. This result indicates that Ni(Cu) solid solution substrates inhibit the rapid growth of IMC at the Sn-Zn/Ni-Cu interface. Ni(Cu) solid solution substrate can also provide various combinations of reaction products at the Sn-Zn/Ni-Cu joints. The Ni₅Zn₂₁ transfers to Ni₂Sn₂Zn + Cu₅Zn₈ phases when the Cu content increased to 60%, and a bi-layered structure Ni₂Sn₂Zn + Cu₅Zn₈ IMCs was formed in Sn-Zn/Ni(Cu) joints at 350 °C regardless of the Cu content in Ni(Cu) substrate (20–80%). These results would provide an effective support in designing Sn-Zn soldering system with optimized IMC layer to improve mechanical performance.

Keywords: interfacial reaction; intermetallic compound; Sn-9Zn solder; Ni(Cu) substrates

1. Introduction

Soldering is one of the most important packaging methods for electronic industry. During soldering, intermetallic compounds (IMCs) form at the solder/substrate interface. A thin, continuous, and uniform IMC layer provides good bonding for soldered joints. The Sn-9Zn (weight percent) alloy, with the melting point of 183 °C, is a promising Pb-free solder because of its environment-friendly, cost-effective, and good mechanical properties [1–4]. Nevertheless, Sn-9Zn alloy tends to form bulky IMC grains at the interface when Sn-9Zn is soldered with common substrates, such as Ni and Cu; however, the soldered Sn-9Zn/Cu and Sn-9Zn/Ni joints presented poor mechanical performance [5–7]. Generally, with the brittle nature of IMC and the tendency to generate structural defects near interface, the bulky IMC grains deteriorate joint reliability [8–11].

Minor alloying elements are added in Sn-9Zn solder to enhance joint reliability. Most studies focused on the alloying effect on Sn-9Zn solder performance; additional elements can enhance the corrosion resistance, tensile strength, and wettability of Sn-9Zn solder [12–17]. Only limited attention was given to interfacial reaction in soldered joints. However, bulky and irregular IMC grains are still formed at the Sn-Zn/Cu interface when Al and Ag are added in the solder [18].

Multielement substrate provides an effective way to change IMC species, morphology, and growth kinetics [19–21]. The interfacial reaction between Ni(Cu) or Ni(Co) multielement substrates, and

Au-20Sn or Sn-Cu solders has been extensively studied [21–24]. Cu alloying in Ni substrate alters the reaction path and induces the formation of thin uniform IMC layers, thereby improving the mechanical reliability of soldered joint [20]. In other words, the mechanical reliability of the joint by using Ni(Cu) substrate to modify the interfacial reaction products is expected to improve. However, only a few publications reported the interfacial reaction between Sn-Zn and Ni(Cu) substrates. To explore the feasibility and implementation of enhancing the reliability of the Sn-Zn soldered joints by using multielement substrates, we carefully investigated the interfacial reactions between Sn-9Zn solder and Ni(Cu) substrate at 250 °C and 350 °C in this study.

2. Materials and Methods

Pure Sn (99.99 wt.%), Zn (99.9 wt.%), Ni (99.99 wt.%), and Cu (99.99 wt.%) shots were carefully weighed to prepare the Sn-9Zn solder and Cu-Ni (20, 40, 60, or 80 at.% Ni) substrates. The Sn-9Zn solder and Ni(Cu) substrates were fabricated by inducing melting in quartz tubes filled with Ar and molten solder casting in the graphite mode. The as-obtained Sn-9Zn and Ni(Cu) plates, with the thickness of 5 mm, were rolled to 0.1 and 1 mm thickness, respectively. The Ni(Cu) was cut into sheets of 5 mm × 5 mm × 1 mm, while Sn-Zn were cut into foils of with the dimension of 5 mm × 5 mm × 0.1 mm.

Before soldering, Ni(Cu) sheets were mechanically polished. The substrate sheets and solder foils were cleaned with acetone in an ultrasonic washer for 5 min. The Sn-9Zn foil was placed between two Ni(Cu) sheets (Figure 1) in a furnace in Ar atmosphere at 250 °C for 1, 4, 9, and 16 h or at 350 °C for 2, 10, and 60 min and then cooled in air.

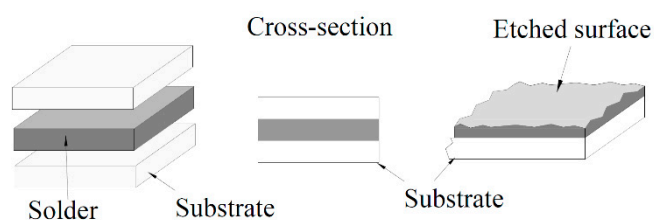


Figure 1. Schematic diagram of Sn-Zn/Ni(Cu) joints.

The soldered samples for electro-probe microanalysis (EPMA) were mechanically polished in the direction normal to the soldering interface. Shimadzu XRD-6000 X-ray diffraction (XRD) instrument, with Cu K α radiation (wavelength 0.154 nm) at 40 kV and a tube current of 30 mA, was used to measure the phase constitution of the reaction layers with the scanning rate of 1 deg/min. To analyze the ternary reaction products accurately, we tensile fractured the soldered joints. Then, the Sn-Zn solder matrix was removed using 5% HCl water solution and cleaned with acetone in an ultrasonic washer for 5 min. The etched surface was perpendicular to cross-section. The etched interfacial microstructure of the joints was further analyzed by scanning electron microscopy (SEM) equipped with an energy dispersive spectrometer.

3. Results and Discussions

3.1. Reaction Products in Sn-Zn/Ni-20Cu Joint

Two reaction layers formed in Sn-Zn/Ni-20Cu joints after soldering at 250 °C Ni-2016 h according to the back-scattered electron (BSE) micrograph (Figure 2a). EPMA result revealed that dark phase-composited Ni-74.7Zn-11.4Cu-1.3Sn (at.%) can be designated as Ni₅Zn₂₁ phase according to Ni-Zn-Cu isothermal section at 250 °C. The reaction product formed between Ni₅Zn₂₁ phase and Ni-20Cu substrate, with the composition of Ni-20.2Zn-7.7Cu-40.8Sn. According to the equilibrium phase diagram of Sn-Zn-Ni and Sn-Zn-Cu system at 250 °C, several ternary phases contained approximately

20 at.% Zn and 40 at.% Sn, as presented in Table 1. It may be a ternary compound, but directly defining the phase constitution only by EPMA measurement is difficult.

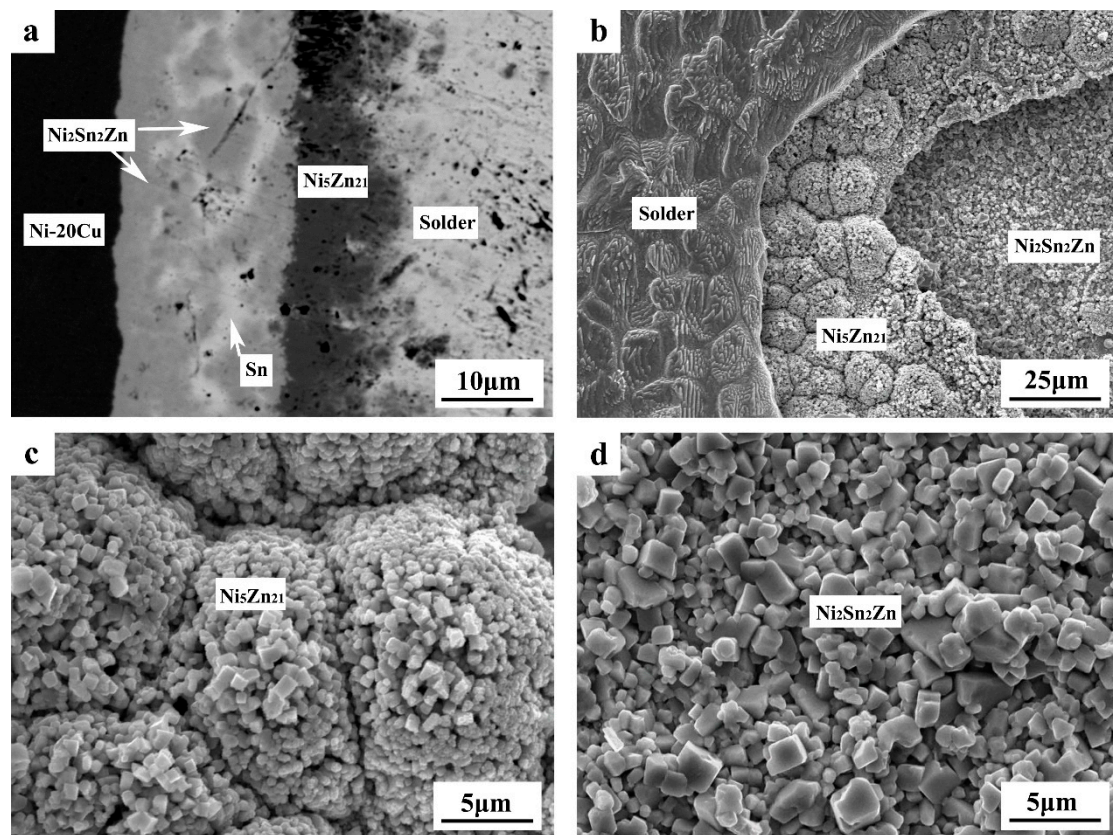


Figure 2. The Sn-Zn/Ni-20Cu joint of 16 h soldering at 250 °C: (a) cross-section micrograph; (b) Etched interface; (c) morphology of $\text{Ni}_5\text{Zn}_{21}$ grains; (d) morphology of $\text{Ni}_2\text{Sn}_2\text{Zn}$ grains.

To analyze the ternary reaction products accurately, we removed the Sn-Zn solder matrix, and the etched surface was further characterized by SEM (FEI Corporation, Hillsboro, OR, USA) and XRD (Rigaku Corporation, Tokyo, Japan). All the three layers, that is, solder matrix, $\text{Ni}_5\text{Zn}_{21}$, and undefined ternary compounds layer, can be directly observed in the etched surface (Figure 2b). The XRD pattern of the etched surface is presented in Figure 3. The Ni-20Cu (PDF, 04-0850), Sn (PDF, 04-0673), and $\text{Ni}_5\text{Zn}_{21}$ (PDF, 04-0850) phases can be identified directly. Other diffraction peaks are identical with the τ_3 phase, as reported by Schmetterer [25], which can be designated as the $\text{Ni}_2\text{Sn}_2\text{Zn}$ phase [26].

Table 1. Ternary phases contained about 20 at.% Zn and 40 at.% Sn found in the system Ni-Sn-Zn [25–31].

Nomenclature	Composition Phase Name			Refs.
	Ni	Sn	Zn	
T1	36.0	38.0	26.0	[27,28]
τ_2	38.5	35.7	25.8	[29]
δ	36.8	38.8	24.4	[30]
τ_1	49.7	36.6	13.7	[30]
δ	31.8	44.5	23.7	[31]
τ_3	33.3	42.8	23.8	[25]
$\text{Ni}_2\text{Sn}_2\text{Zn}$	40.0	40.0	20.0	[26]

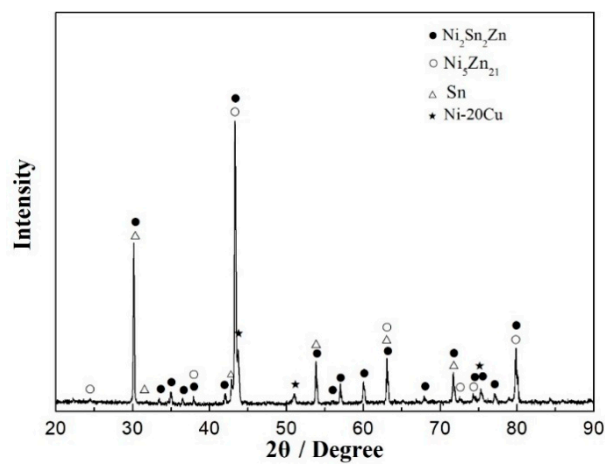


Figure 3. The X-ray diffraction (XRD) pattern of etched interface of Sn-Zn/Ni-20Cu joint after soldered at 250 °C for 16 h.

Figure 4 illustrates the BSE micrographs and XRD patterns of Sn-Zn/Ni-20Cu couple after reaction at 250 °C for 1 and 9 h. Only a $\text{Ni}_5\text{Zn}_{21}$ layer formed at the interface after 9 h of soldering. The loose $\text{Ni}_5\text{Zn}_{21}$ layer was formed at the interface after 1 h of soldering. Meanwhile, after 9 h, a dense $\text{Ni}_5\text{Zn}_{21}$ layer was formed.

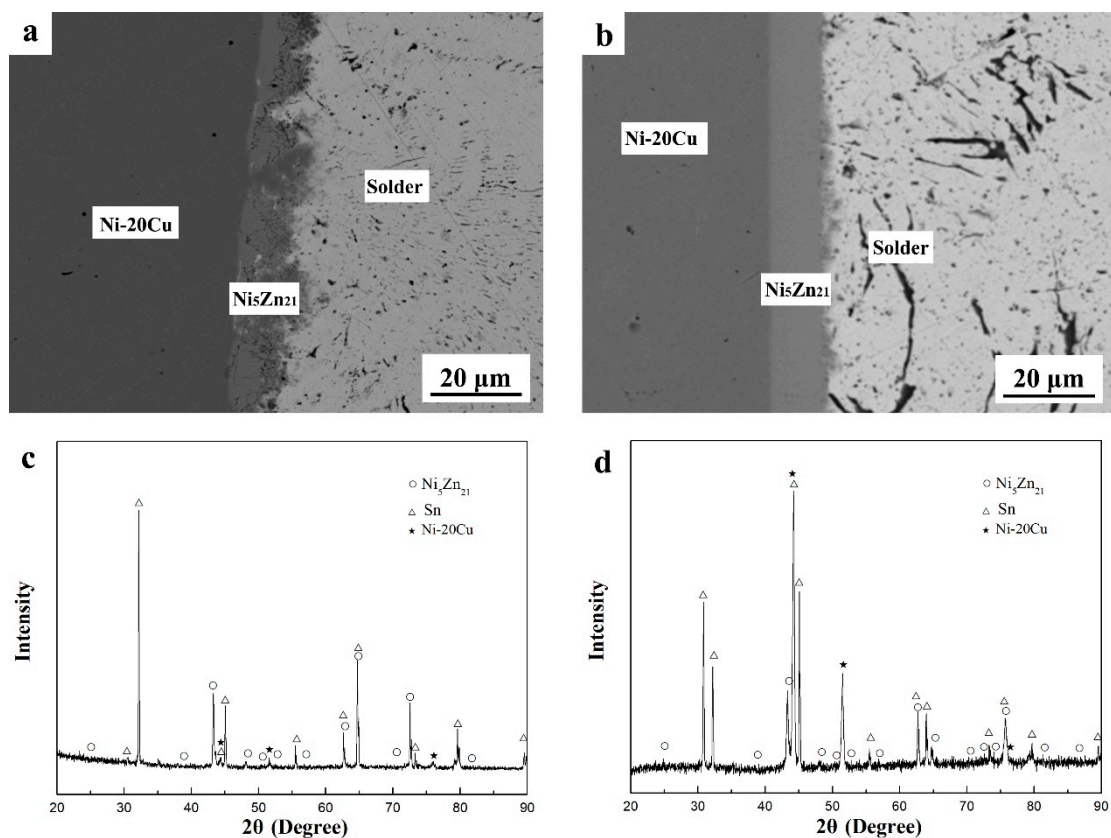


Figure 4. Cross-section micrographs (a,b) and X-ray diffraction (XRD) patterns (c,d) of Sn-Zn/Ni-20Cu joints after soldered at 250 °C for 1 h (a,c) and 9 h (b,d).

3.2. Effect of Cu Content on Reaction Products

Figure 5 shows the BSE micrographs and XRD patterns of Sn-Zn/Ni-Cu couples after reaction at 250 °C for 9 h, and the compositions of each reaction products are listed in Table 2. As shown in the table,

the Cu content in the substrate exerted considerable effect on the interfacial reaction products. When Sn-9Zn solder reacted with Ni-40Cu substrate, a uniform Ni_5Zn_{21} layer was formed at the interface. However, two reaction layers, namely, Ni_2Sn_2Zn and Cu_5Zn_8 , were formed in Sn-Zn/Ni-60Cu, and Cu_5Zn_8 and CuZn layers appeared in Sn-Zn/Ni-80Cu.

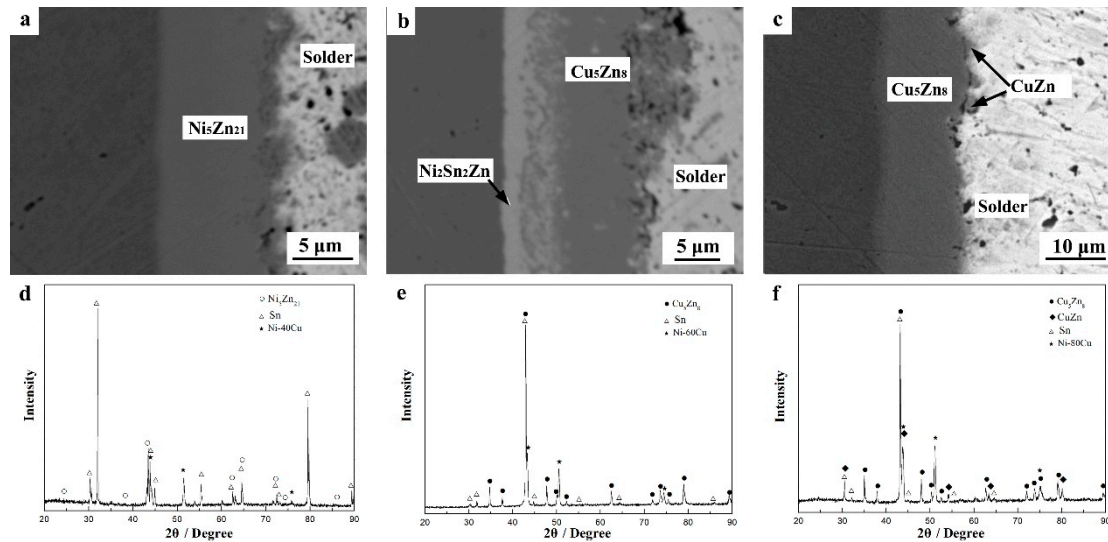


Figure 5. Cross-section micrographs and X-ray diffraction (XRD) patterns of etched interface of joints after soldered 9 h at 250 °C: (a,d) Sn-Zn/Ni-40Cu; (b,e) Sn-Zn/Ni-60Cu; (c,f) Sn-Zn/Ni-80Cu.

Table 2. The composition of reaction products in Sn-Zn/Ni-Cu joints after soldered at 250 °C for 9 h.

Substrate	Compositions (at.%)				Phase
	Ni	Cu	Sn	Zn	
Ni-20Cu	16.44	1.98	1.45	80.13	Ni_5Zn_{21}
Ni-40Cu	14.94	9.25	0.31	75.50	Ni_5Zn_{21}
Ni-60Cu	26.12	16.91	41.95	15.01	Ni_2Sn_2Zn
	8.87	21.74	1.75	67.64	Cu_5Zn_8
Ni-80Cu	5.61	27.97	1.24	65.17	Cu_5Zn_8
	5.17	35.32	8.43	51.08	CuZn

Cu content in substrate also altered the morphology of the products. Figure 6 illustrates the etched surface of Sn-Zn/Ni-Cu joint after reaction at 250 °C for 9 h. In the Ni_5Zn_{21} phase in Sn-Zn/Ni-20Cu and Sn-Zn/Ni-40Cu joints, extremely fine Ni_5Zn_{21} grains constituted the layer in Sn-Zn/Ni-20Cu joint, and the spherical Ni_5Zn_{21} particles formed at interface in Sn-Zn/Ni-40Cu joints. A dense Cu_5Zn_8 layer was formed in the Sn-Zn/Ni-60Cu joint, while a dense Cu_5Zn_8 layer with some CuZn grains was formed in the Sn-Zn/Ni-80Cu joint.

The solid solution element in reaction IMCs played a significant role in IMC morphology. As reported in most references, bulky Cu_5Zn_8 grains are formed in the Sn-Zn/Cu joint during long reaction time, which extremely deteriorates the joint reliability [5,11]. However, the fine-grained Cu_5Zn_8 layer was formed in Sn-Zn/Ni-60Cu and Sn-Zn/Ni-80Cu joints when 5–9 at.% Ni was dissolved in the Cu_5Zn_8 phase.

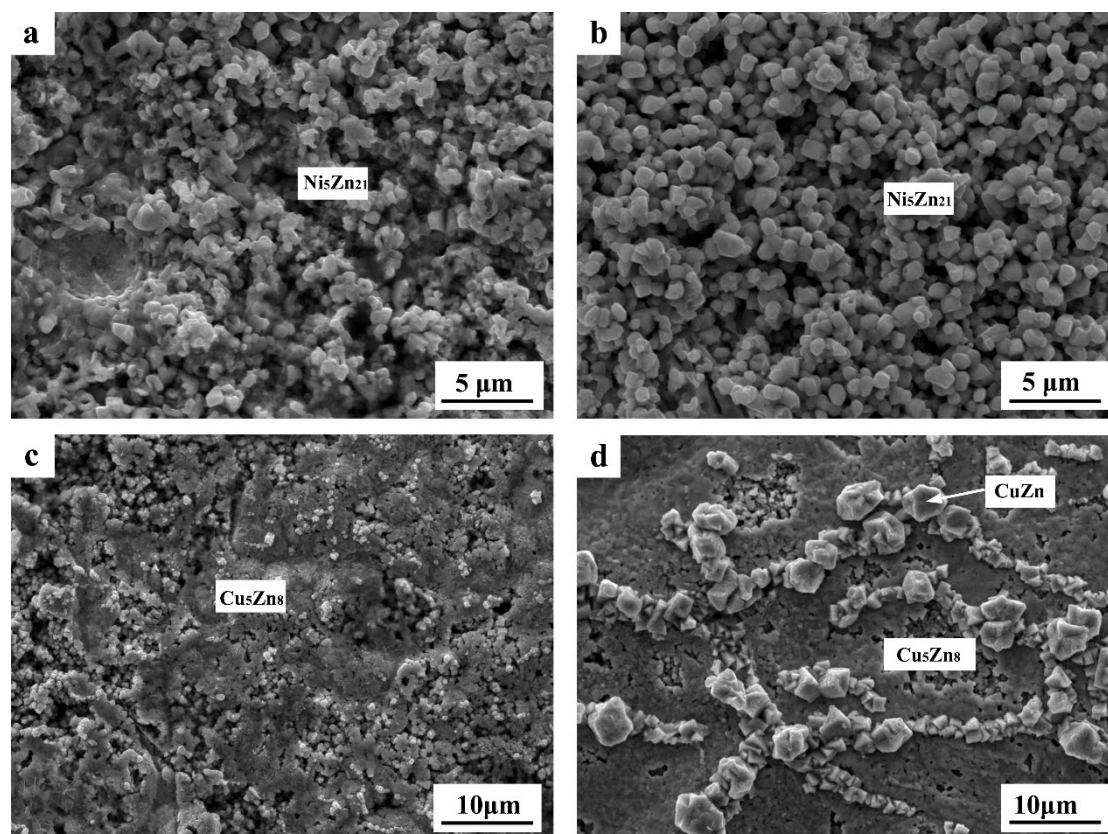


Figure 6. Etched surface micrograph of joints after soldered 9 h at 250 °C: (a) Sn-Zn/Ni-20Cu; (b) Sn-Zn/Ni-40Cu; (c) Sn-Zn/Ni-60Cu; (d) Sn-Zn/Ni-80Cu.

Table 3 summarizes the interfacial reaction products of Sn-Zn/Ni-Cu after soldering at 250 °C for various durations. Hence, $\text{Ni}_5\text{Zn}_{21}$ is the first formed product in Ni-20Cu and Ni-40Cu joints, whereas the Cu_5Zn_8 phase is the first formed product in Ni-60Cu and Ni-80Cu joints. After prolonging the reaction time, $\text{Ni}_2\text{Sn}_2\text{Zn}$ phase was formed between the first formed product and substrate. $\text{Ni}_2\text{Sn}_2\text{Zn}$ was formed in Sn-Zn/Ni-60Cu joint only after 1 h of soldering but appeared in all joints after 16 h.

Table 3. Interfacial reaction products of Sn-Zn/Ni-Cu after various durations at 250 °C.

Substrates	Soldering Time (h)			
	1	4	9	16
Ni-20Cu	$\text{Ni}_5\text{Zn}_{21}$	$\text{Ni}_5\text{Zn}_{21}$	$\text{Ni}_5\text{Zn}_{21}$	$\text{Ni}_2\text{Sn}_2\text{Zn} + \text{Ni}_5\text{Zn}_{21}$
Ni-40Cu	$\text{Ni}_5\text{Zn}_{21}$	$\text{Ni}_5\text{Zn}_{21}$	$\text{Ni}_5\text{Zn}_{21}$	$\text{Ni}_2\text{Sn}_2\text{Zn} + \text{Ni}_5\text{Zn}_{21}$
Ni-60Cu	$\text{Ni}_2\text{Sn}_2\text{Zn} + \text{Cu}_5\text{Zn}_8$	$\text{Ni}_2\text{Sn}_2\text{Zn} + \text{Cu}_5\text{Zn}_8$	$\text{Ni}_2\text{Sn}_2\text{Zn} + \text{Cu}_5\text{Zn}_8$	$\text{Ni}_2\text{Sn}_2\text{Zn} + \text{CuZn}$
Ni-80Cu	Cu_5Zn_8	Cu_5Zn_8	$\text{Cu}_5\text{Zn}_8 + \text{CuZn}$	$\text{Ni}_2\text{Sn}_2\text{Zn} + \text{CuZn}$

3.3. Effect of Soldering Temperature on Reaction Products

When the soldering temperature increased to 350 °C, $\text{Ni}_2\text{Sn}_2\text{Zn} + \text{Cu}_5\text{Zn}_8$ phases appeared at the interface regardless of the Cu content in Ni-Cu substrates after short soldering time, that is, 2 min (Figure 7). Nevertheless, the volume fraction of Cu_5Zn_8 increased with the increase in Cu content in the substrate. Only few Cu_5Zn_8 grains appeared in the Sn-Zn/Ni-20Cu and Sn-Zn/Ni-40Cu joints, but a Cu_5Zn_8 layer occurred between $\text{Ni}_2\text{Sn}_2\text{Zn}$ and solder matrix when the Cu content in the substrate was >60%.

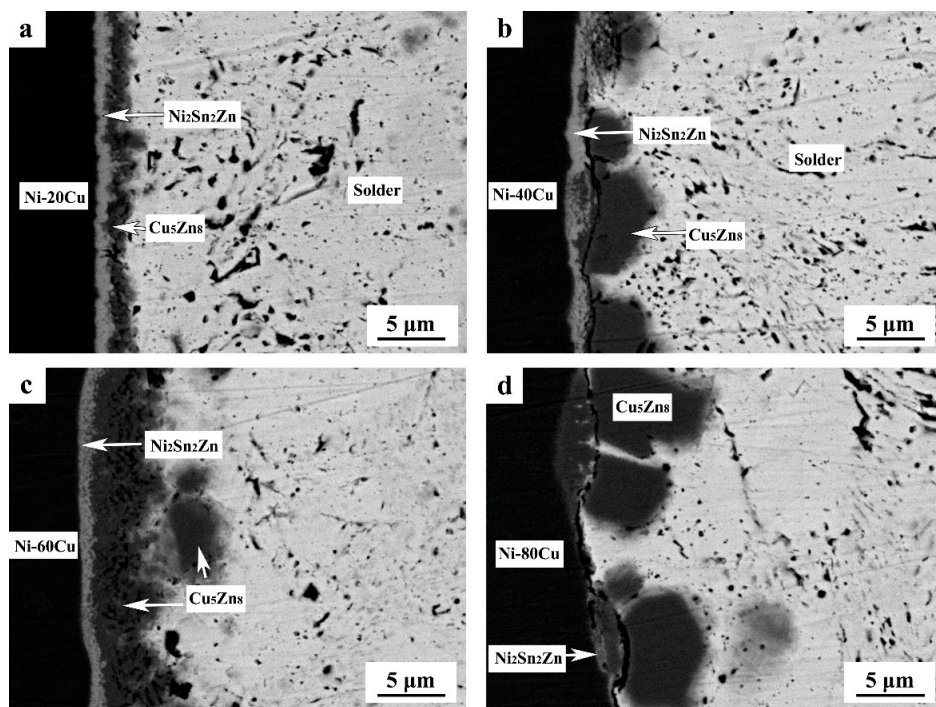


Figure 7. Cross-section micrograph of joints after soldered 2 min at 350 °C: (a) Sn-Zn/Ni-20Cu; (b) Sn-Zn/Ni-40Cu; (c) Sn-Zn/Ni-60Cu; (d) Sn-Zn/Ni-80Cu.

Figure 8 presents the interfacial reaction products of Sn-Zn/Ni-Cu joints after soldering at 350 °C for 60 min. Ni_3Sn_4 phase formed at the Sn-Zn/Ni-20Cu interface, while mainly $\text{Ni}_2\text{Sn}_2\text{Zn}$ phase was formed when Cu content in the substrate was >20%. CuZn grains also appeared in Sn-Zn/Ni-60Cu and Sn-Zn/Ni-80Cu joints. The interfacial reaction products in Sn-Zn/Ni-Cu joints after various durations at 350 °C are listed in Table 4.

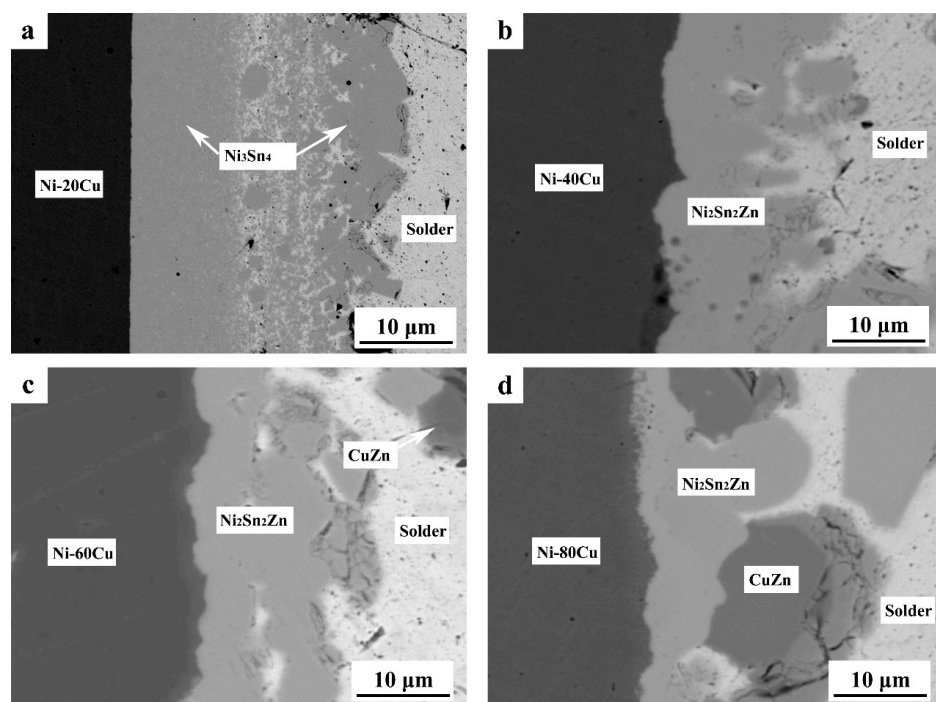


Figure 8. Cross-section micrograph of joints after soldered 60 min at 350 °C: (a) Sn-Zn/Ni-20Cu; (b) Sn-Zn/Ni-40Cu; (c) Sn-Zn/Ni-60Cu; (d) Sn-Zn/Ni-80Cu.

Table 4. Interfacial reaction products of Sn-Zn/Ni-Cu after various durations at 350 °C.

Substrates	Soldering Time		
	2 min	10 min	60 min
Ni-20Cu	$\text{Ni}_2\text{Sn}_2\text{Zn} + \text{Cu}_5\text{Zn}_8$	$\text{Ni}_2\text{Sn}_2\text{Zn} + \text{Cu}_5\text{Zn}_8$	Ni_3Sn_4
Ni-40Cu	$\text{Ni}_2\text{Sn}_2\text{Zn} + \text{Cu}_5\text{Zn}_8$	$\text{Ni}_2\text{Sn}_2\text{Zn} + \text{Cu}_5\text{Zn}_8$	$\text{Ni}_2\text{Sn}_2\text{Zn}$
Ni-60Cu	$\text{Ni}_2\text{Sn}_2\text{Zn} + \text{Cu}_5\text{Zn}_8$	$\text{Ni}_2\text{Sn}_2\text{Zn} + \text{Cu}_5\text{Zn}_8$	$\text{Ni}_2\text{Sn}_2\text{Zn} + \text{CuZn}$
Ni-80Cu	$\text{Ni}_2\text{Sn}_2\text{Zn} + \text{Cu}_5\text{Zn}_8$	$\text{Ni}_2\text{Sn}_2\text{Zn} + \text{Cu}_5\text{Zn}_8$	$\text{Ni}_2\text{Sn}_2\text{Zn} + \text{CuZn}$

3.4. Discussions

It is generally accepted that joint reaction occurs in two steps: (1) solidification preceded by the substrate dissolution; and (2) some transformations in the solid [32,33]. Considering the evolution of interfacial microstructure, two reaction stages can be roughly determined for the interfacial reaction between Sn-Zn solder and Ni-Cu substrate, as demonstrated in Figures 9 and 10. Given that no quaternary phase in Zn-Sn-Ni-Cu system has been reported or detected thus far, the possible reaction paths of Sn-9Zn/Ni-Cu couples were proposed according to the Ni-Sn-Zn [25–31] and Cu-Sn-Zn [34] isothermal sections at 250 and 350 °C, and no other phases were suspended. In addition, the reactions are peritectic reaction according to the Ni-Sn-Zn [25–31] and Cu-Sn-Zn [34] phase diagram at 250 and 350 °C. The solid substrates or reaction product react with liquid and form new reaction products.

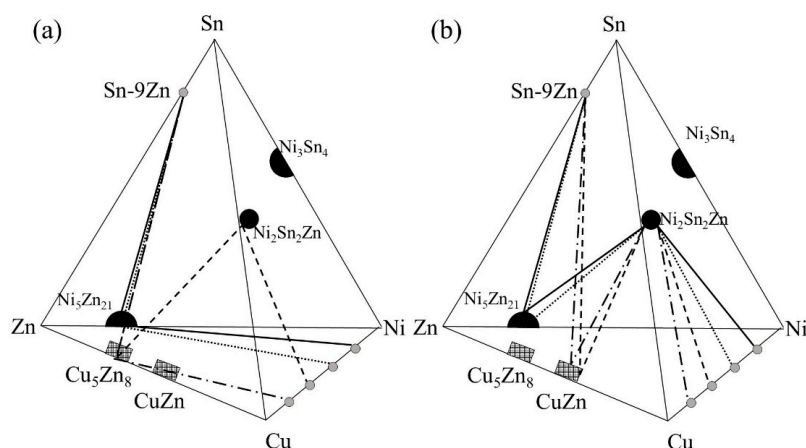


Figure 9. Two reaction stages of the Sn-Zn/Ni(Cu) joints superimpose on the Zn-Sn-Ni-Cu isothermal tetrahedron at 250 °C during (a) early stage; and (b) later stage.

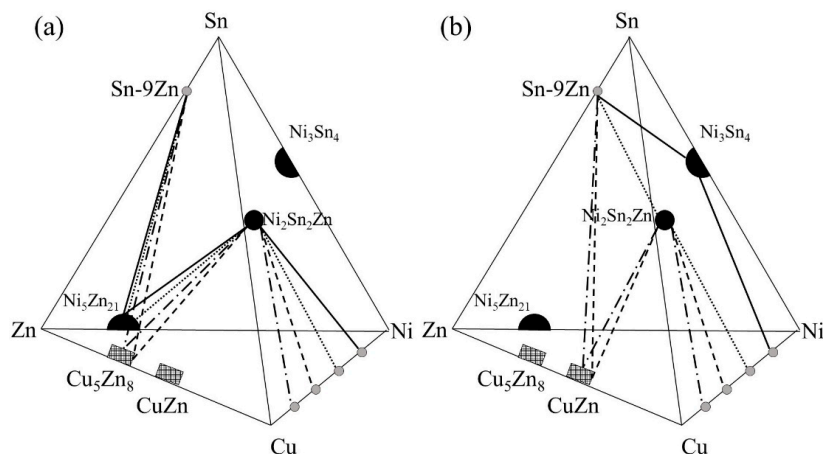


Figure 10. Two reaction stages of the Sn-Zn/Ni(Cu) joints superimpose on the Zn-Sn-Ni-Cu isothermal tetrahedron at 350 °C during (a) early stage; and (b) later stage.

The monolayered IMC structure appeared first after soldering at 250 °C. Meanwhile, bi-layered IMC structure was observed at 350 °C. As listed in Tables 3 and 4, Ni₅Zn₂₁ was the first formed product in Ni-20Cu and Ni-40Cu joints, whereas Ni₂Sn₂Zn + Cu₅Zn₈ phases in Ni-60Cu and Cu₅Zn₈ phase in Ni-80Cu. However, Ni₂Sn₂Zn + Cu₅Zn₈ phases were always formed at 350 °C as it always had Cu content in Ni(Cu) substrate (20–80%).

Thermodynamic and kinetic factors determine the interfacial reaction products during soldering process [35]. The reaction products generally tend to be controlled by the diffusivity of the reactant in the reaction zone [10]. In most cases, only an IMC layer forms at the interface at first, even when solder reacts with binary substrate, because one element in substrate would dominate the interfacial reaction. For example, Ni is the dominant reaction element in Ni-20Cu and Ni-40Cu substrates when soldering at 250 °C. Similar to the reaction product formed in the Sn-Zn/Ni joint [21,36], Ni₅Zn₂₁ is still the first formed product in the Sn-Zn/Ni-20Cu and Sn-Zn/Ni-40Cu joints.

By contrast, if both elements in the binary substrate can provide successive supplement toward the reaction zone, then a bi-layered IMC structure would occur at first. The diffusivity of reactants in the reaction zone was dependent upon the content and temperature. The Ni₂Sn₂Zn + Cu₅Zn₈ bi-layered IMC structure only appeared in the Sn-Zn/Ni-60Cu joint after soldering at 250 °C. This result indicated that binary substrate with suitable content can provide successive supplement of both elements toward the reaction zone. This suitable substrate composition range would increase with the increment of soldering temperature. Given that the diffusion coefficient of atomic will dramatically increase with increased temperature, the Ni₂Sn₂Zn + Cu₅Zn₈ bi-layer was formed first at 350 °C when the Cu content in the Ni-Cu substrate ranged from 20% to 80%.

The new reaction products (mainly Ni₂Sn₂Zn) occurred when soldering time was prolonged; thus, the original reaction product is no longer in local equilibrium after reacting at a sufficiently long time [24,37]. The formation of Ni₂Sn₂Zn phase between Ni and Ni₅Zn₂₁ was also reported in Sn-Zn/Ni joint after prolonged soldering time [15]. In the present work, the Zn in solder is depleted in a later reaction stage, while the products formed in the early stage react with liquid solder (mainly Sn) and new phases appear. The Ni₅Zn₂₁ phase transferred to Ni₂Sn₂Zn, and Cu₅Zn₈ phase transferred to Ni₂Sn₂Zn and CuZn when the reaction time at 250 °C was prolonged.

In brief, when soldering with Sn-Zn solder, Ni(Cu) solid solution substrate can optimize the morphologies of Ni₅Zn₂₁ and Cu₅Zn₈ at the interface, and a thin and uniform reaction layer consisting of fine IMC grains can be obtained. Various reaction product combinations were formed at the interface, that is, Ni₂Sn₂Zn + Cu₅Zn₈. The formation of thin Ni₂Sn₂Zn layer near the substrate enhances the joint reliability [15]. Hence, the adoption of Ni(Cu) solid solution substrate will provide an effective way to improve the joint reliability of the Sn-Zn soldering system.

4. Conclusions

1. When soldered at 250 °C, fine-grained Ni₅Zn₂₁ was the first formed product in Sn-Zn/Ni-20Cu and Sn-Zn/Ni-40Cu joints, while Ni₂Sn₂Zn + Cu₅Zn₈ and fine-grained Cu₅Zn₈ phases were formed in Sn-Zn/Ni-60Cu and Sn-Zn/Ni-80Cu joints, respectively. Ni₅Zn₂₁ layer transferred to Ni₂Sn₂Zn phase, whereas Cu₅Zn₈ phase transferred to Ni₂Sn₂Zn and CuZn phases at prolonged reaction time.
2. Ni₂Sn₂Zn + Cu₅Zn₈ bi-layered structure was always formed first in Sn-Zn/Ni(Cu) joint at 350 °C regardless of the Cu content in Ni(Cu) substrate (20–80%). However, the bi-layered Ni₂Sn₂Zn + Cu₅Zn₈ transferred to a loose Ni₃Sn₄ layer in the Sn-Zn/Ni-20Cu joint, whereas a Ni₂Sn₂Zn layer transferred in Sn-Zn/Ni-40Cu joint. Meanwhile, Ni₂Sn₂Zn and CuZn transferred in Sn-Zn/Ni-60Cu and Sn-Zn/Ni-80Cu joints when the reaction time was prolonged at 350 °C.
3. Using Ni(Cu) solid solution substrates, the morphologies of Ni₅Zn₂₁ and Cu₅Zn₈ can be optimized, and various reaction product combinations can be obtained at the interface. These results would provide an effective way to improve the joint reliability of the Sn-Zn soldering system.

Author Contributions: Research program design, writing—review and editing, X.Z.; data collection and analysis, writing—original draft preparation, J.P.; provided guidance and assistance in the experiments, X.W.; participates in research and data collection, P.Y. and F.W.

Funding: This research was funded by the Shaanxi Province Science and Technology Key Project, grant number 2016NY-137, the Fundamental Research Funds for the Central Universities, grant number 2452017132, 2452016075 and the National Major Science and Technology Project of China, grant number 2017YFB0305700.

Conflicts of Interest: The authors declare no conflicts of interest.

References

1. Guo, W.; Luan, T.; He, J.; Yan, J. Ultrasonic-assisted soldering of fine-grained 7034 aluminum alloy using Sn-Zn solders below 300 °C. *Ultrason. Sonochem.* **2018**, *40*, 815–821. [[CrossRef](#)] [[PubMed](#)]
2. Luan, T.; Guo, W.; Yang, S.; Ma, Z.; He, J.; Yan, J. Effect of intermetallic compounds on mechanical properties of copper joints ultrasonic-soldered with Sn-Zn alloy. *J. Mater. Process. Technol.* **2017**, *248*, 123–129. [[CrossRef](#)]
3. Zhang, L.; Xue, S.B.; Gao, L.L.; Sheng, Z.; Ye, H.; Xiao, Z.X.; Zeng, G.; Chen, Y.; Yu, S.L. Development of Sn-Zn lead-free solders bearing alloying elements. *J. Mater. Sci. -Mater. Electron.* **2009**, *21*, 1–15. [[CrossRef](#)]
4. Liou, W.-k.; Yen, Y.-W.; Jao, C.-C. Interfacial Reactions of Sn-9Zn-xCu ($x = 1, 4, 7, 10$) Solders with Ni Substrates. *J. Electron. Mater.* **2009**, *38*, 2222–2227. [[CrossRef](#)]
5. Zhao, N.; Zhong, Y.; Huang, M.L.; Dong, W.; Ma, H.T.; Wang, Y.P. In situ study on interfacial reactions of Cu/Sn-9Zn/Cu solder joints under temperature gradient. *J. Alloys Compd.* **2016**, *682*, 1–6. [[CrossRef](#)]
6. Yoon, J.-W.; Jung, S.-B. Reliability studies of Sn-9Zn/Cu solder joints with aging treatment. *J. Alloys Compd.* **2006**, *407*, 141–149. [[CrossRef](#)]
7. Zhu, W.; Liu, H.; Wang, J.; Ma, G.; Jin, Z. Interfacial Reactions Between Sn-Zn Alloys and Ni Substrates. *J. Electron. Mater.* **2009**, *39*, 209–214. [[CrossRef](#)]
8. Laurila, T.; Vuorinen, V.; Kivilahti, J.K. Interfacial reactions between lead-free solders and common base materials. *Mater. Sci. Eng. R Rep.* **2005**, *49*, 1–60. [[CrossRef](#)]
9. Tu, K.; Liu, Y. Recent advances on kinetic analysis of solder joint reactions in 3D IC packaging technology. *Mater. Sci. Eng. R Rep.* **2019**, *136*, 1–12. [[CrossRef](#)]
10. Kao, C.R.; Chang, Y.A. A theoretical analysis for the formation of periodic layered structure in ternary diffusion couples involving a displacement type of reactions. *Acta Metall. Mater.* **1993**, *41*, 3463–3472. [[CrossRef](#)]
11. Wang, J.Y.; Lin, C.F.; Chen, C.M. Retarding the Cu₅Zn₈ phase fracture at the Sn-9wt.% Zn/Cu interface. *Scr. Mater.* **2011**, *64*, 633–636. [[CrossRef](#)]
12. Liu, J.-C.; Wang, Z.-H.; Xie, J.-Y.; Ma, J.-S.; Shi, Q.-Y.; Zhang, G.; Suganuma, K. Effects of intermetallic-forming element additions on microstructure and corrosion behavior of Sn-Zn solder alloys. *Corros. Sci.* **2016**, *112*, 150–159. [[CrossRef](#)]
13. Liu, J.-C.; Zhang, G.; Ma, J.-S.; Suganuma, K. Ti addition to enhance corrosion resistance of Sn-Zn solder alloy by tailoring microstructure. *J. Alloys Compd.* **2015**, *644*, 113–118. [[CrossRef](#)]
14. Hu, Y.-h.; Xue, S.-b.; Wang, H.; Ye, H.; Xiao, Z.-x.; Gao, L.-l. Effects of rare earth element Nd on the solderability and microstructure of Sn-Zn lead-free solder. *J. Mater. Sci. -Mater. Electron.* **2010**, *22*, 481–487. [[CrossRef](#)]
15. Li, J.; Peng, J.; Wang, R.; Feng, Y.; Peng, C. Effects of Co addition on shear strength and interfacial microstructure of Sn-Zn-(Co)/Ni joints. *J. Mater. Sci. -Mater. Electron.* **2018**, *29*, 19901–19908. [[CrossRef](#)]
16. Ren, G.; Wilding, I.J.; Collins, M.N. Alloying influences on low melt temperature SnZn and SnBi solder alloys for electronic interconnections. *J. Alloys Compd.* **2016**, *665*, 251–260. [[CrossRef](#)]
17. Huang, Y.C.; Chen, S.W. Co alloying and size effects on solidification and interfacial reactions in the Sn-Zn-(Co)/Cu couples. *J. Mater. Res.* **2010**, *25*, 2430–2438. [[CrossRef](#)]
18. Huang, M.; Hou, X.; Kang, N.; Yang, Y. Microstructure and interfacial reaction of Sn-Zn-X (Al, Ag) near-eutectic solders on Al and Cu substrates. *J. Mater. Sci. -Mater. Electron.* **2014**, *25*, 2311–2319. [[CrossRef](#)]
19. Maeshima, T.; Ikehata, H.; Terui, K.; Sakamoto, Y. Effect of Ni to the Cu substrate on the interfacial reaction with Sn-Cu solder. *Mater. Des.* **2016**, *103*, 106–113. [[CrossRef](#)]
20. Peng, J.; Wang, R.C.; Wang, M.; Liu, H.S. Interfacial Microstructure Evolution and Shear Behavior of Au-Sn/Ni-xCu Joints at 350 °C. *J. Electron. Mater.* **2017**, *46*, 2021–2029. [[CrossRef](#)]

21. Lin, H.-f.; Chang, Y.-c.; Chen, C.-c. Sn-Zn/Ni-Co Interfacial Reactions at 250 °C. *J. Electron. Mater.* **2014**, *43*, 3333–3340. [[CrossRef](#)]
22. Huang, K.C.; Shieu, F.S.; Huang, T.S.; Lu, C.T.; Chen, C.W.; Tseng, H.W.; Cheng, S.L.; Liu, C.Y. Study of Interfacial Reactions Between Sn(Cu) Solders and Ni-Co Alloy Layers. *J. Electron. Mater.* **2010**, *39*, 2403–2411. [[CrossRef](#)]
23. Chen, C.-C.; Chan, Y.-T.; Chen, Y.-T. Interfacial reactions between Sn-Cu solders and Ni-Co alloys at 250 °C. *Int. J. Mater. Res.* **2011**, *25*, 1321–1328. [[CrossRef](#)]
24. Chen, C.-c.; Chen, Y.-t. Alternating reaction phases in Sn-Cu/Ni-Co solid-state reactions. *J. Alloys Compd.* **2012**, *545*, 28–31. [[CrossRef](#)]
25. Schmetterer, C.; Rajamohan, D.; Ipser, H.; Flandorfer, H. The high-temperature phase equilibria of the Ni-Sn-Zn system: Isothermal sections. *Intermetallics* **2011**, *19*, 1489–1501. [[CrossRef](#)] [[PubMed](#)]
26. Schmetterer, C.; Rajamohan, D.; Effenberger, H.S.; Flandorfer, H. Ni₂Sn₂Zn from single-crystal X-ray diffraction. *Acta Crystallogr. Sect. C Cryst. Struct. Commun.* **2012**, *68*, i65–i67. [[CrossRef](#)]
27. Gandova, V.; Soares, D.; Lilova, K.; Tedenac, J.C.; Vassilev, G.P. Phase equilibria in the Sn-Zn-Ni system. *Int. J. Mater. Res.* **2011**, *102*, 257. [[CrossRef](#)]
28. Gandova, V.; Vassilev, G.P. Thermodynamic optimization and phase equilibria in the ternary system Ni-Sn-Zn. *J. Alloys Compd.* **2014**, *609*, 1–6. [[CrossRef](#)]
29. Chang, J.; Seo, S.-K.; Lee, H.M. Phase Equilibria in the Sn-Ni-Zn Ternary System: Isothermal Sections at 200 °C, 500 °C, and 800 °C. *J. Electron. Mater.* **2010**, *39*, 2643–2652. [[CrossRef](#)]
30. Liang, J.-L.; Du, Y.; Tang, Y.-Y.; Xie, S.-B.; Xu, H.-H.; Zeng, L.-M.; Liu, Y.; Zhu, Q.-M.; Nong, L.-Q. Phase Equilibria in the Ni-Sn-Zn System at 500 °C. *J. Electron. Mater.* **2011**, *40*, 2290–2299. [[CrossRef](#)]
31. Chen, S.-w.; Hsu, C.-m.; Chou, C.-y.; Hsu, C.-w. Isothermal section of ternary Sn-Zn-Ni phase equilibria at 250 °C. *Prog. Nat. Sci. Mater. Int.* **2011**, *21*, 386–391. [[CrossRef](#)]
32. Wołczyński, W.; Okane, T.; Senderowski, C.; Zasada, D.; Kania, B.; Janczak-Rusch, J. Thermodynamic justification for the Ni/Al/Ni joint formation by a diffusion brazing. *Int. J. Thermodyn.* **2011**, *14*, 97–105. [[CrossRef](#)]
33. Wołczyński, W.; Okane, T.; Senderowski, C.; Kania, B.; Zasada, D.; Janczak-Rusch, J. Meta-stable conditions of diffusion brazing. *Arch. Metall. Mater.* **2011**, *56*, 311–323. [[CrossRef](#)]
34. Huang, Y.-c.; Chen, S.-w.; Chou, C.-y.; Gierlotka, W. Liquidus projection and thermodynamic modeling of Sn-Zn-Cu ternary system. *J. Alloys Compd.* **2009**, *477*, 283–290. [[CrossRef](#)]
35. Sun, Y.; Liu, H.; Xie, Z.; Jin, Z. Prediction of interfacial reaction products between metals with same lattice structure through thermodynamic modeling. *CALPHAD* **2016**, *52*, 180–185. [[CrossRef](#)]
36. Chan, Y.C.; Chiu, M.Y.; Chuang, T.H. Intermetallic Compounds Formed during the Soldering Reactions of Eutectic Sn-9Zn with Cu and Ni Substrates. *Zeitschrift Für Metallkunde* **2002**, *93*, 95–98. [[CrossRef](#)]
37. Chen, W.M.; Yang, S.C.; Tsai, M.H.; Kao, C.R. Uncovering the driving force for massive spalling in the Sn-Cu/Ni system. *Scr. Mater.* **2010**, *63*, 47–49. [[CrossRef](#)]

